ISSN 1063-7761, Journal of Experimental and Theoretical Physics, 2020, Vol. 130, No. 5, pp. 690–698. © Pleiades Publishing, Inc., 2020.
Russian Text © The Author(s), 2020, published in Zhurnal Eksperimental'noi i Teoreticheskoi Fiziki, 2020, Vol. 157, No. 5, pp. 824–833.

ORDER, DISORDER, AND PHASE TRANSITION IN CONDENSED SYSTEM

Spin State of the Co^{3+} Ions in the Layered $TbBaCo_2O_{5.5}$ Cobaltite in the Metal–Insulator Transition Range

N. I. Solin[a],*, S. V. Naumov[a], and V. A. Kazantsev[a]

[a] *Mikheev Institute of Metal Physics, Ural Branch, Russian Academy of Sciences, Yekaterinburg, 620108 Russia*

**e-mail: solin@imp.uran.ru*

Received June 19, 2019; revised November 22, 2019; accepted December 10, 2019

Abstract—A scheme is proposed to describe the spin state of the Co^{3+} ions in the layered $TbBaCo_2O_{5.5}$ cobaltite near the metal–insulator transition. The spin state of the Co^{3+} ions in the metallic phase corresponds to a mixture of the HS($t_{2g}^4\ e_g^2$, $S = 2$) and LS($t_{2g}^6\ e_g^0$, $S = 0$) states taken at approximately the same proportion. The transition into a nonmetallic state occurs due to the transformation of the HS state into the LS state in octahedra and part of the LS state into the IS($t_{2g}^5\ e_g^1$, $S = 1$) state in pyramids (near $T_C \sim 280$ K). The proposed scheme agrees with the well-known structural data obtained for the $TbBaCo_2O_{5.5}$ cobaltites. As follows from volumetric and linear expansion, the transition takes place over a wide temperature range $T \approx T_{MI} \pm 50$ K. The study of thermal expansion shows that an LS/IS state is retained down to $T = 80$ K.

DOI: 10.1134/S1063776120050106

INTRODUCTION

Interest in the ordered layered $RBaCo_2O_{5+\delta}$ cobalt oxides is mainly caused by the detection of colossal magnetoresistance (MR) in hole lanthanum manganites [1, 2]. Although they do not exhibit the magnetoresistance properties comparable with those of hole manganites, they attract great attention due to their unusual magnetic and electrical properties and phase transitions [3–15]. The driving force of the cation ordering in the $R_{1-x}Ba_xCoO_{3-\delta}$ perovskites at $x = 0.5$ is the significant difference between the radii of the R^{3+} and Ba^{3+} rare-earth ions, which leads to cation ordering in the form of alternating layers with rare-earth (R) and alkali metal (Ba) ions. The layered $RBaCo_2O_{5+\delta}$ cobaltites have a perovskite crystal structure, in which RO and BaO layers alternate with CoO_2 layers located normal to axis *c*. They are strongly anisotropic because of their layered structure [3, 11]. Depending on the oxygen content $0 \le \delta \le 1$, the valence state of cobalt changes from Co^{2+} to Co^{4+}, and Co ions have different oxygen environment (octahedra or pyramids with a square base). $RBaCo_2O_{5.5}$ only contains Co^{3+} ions, which are located in the crystal lattice of the same number of CoO_6 octahedra and square CoO_5 pyramids, and the oxygen pyramids and octahedra surrounding Co^{3+} ions are ordered [2].

The unusual electron, magnetic, and structural transitions in $RBaCo_2O_{5+\delta}$, $\delta \approx 0.5$, are of particular interest. The following sequential transitions were detected in them: metal–insulator (MI), paramagnetic (PM), ferromagnetic (FM), and antiferromagnetic (AFM) transitions [1–15]. In contrast to manganites, the MI transition in cobaltites is not related to magnetic ordering, which results from the magnetically active (antiferromagnetic) character of the $RMnO_3$ matrix in the case of manganites and the weakly magnetic (paramagnetic) behavior of $RCoO_3$ in the case of cobaltites (as the nature of magnetoresistance). Colossal magnetoresistance is promoted by the presence of FM clusters in an AFM matrix. The FM clusters in hole manganites are coupled to an AFM matrix by an exchange interaction, which causes an increase in the cluster size and a high MR [16, 17]. The increase in the magnetic cluster (polaron) size with decreasing temperature or in a magnetic field is explained by the unusual transport properties of layered manganites, namely, metal–nonmetal transition and higher MR [18]. A weakly magnetic cobaltite matrix exhibits cluster coalescence [19] and a low MR. The properties of the matrix cause the following new phenomena for layered cobalt oxides: a unidirectional electrical resistance anisotropy, exchange bias [20, 21], and the absence of exchange bias in MR hole manganites.

The physics of layered cobaltites is determined by the complex interaction between the charge, spin, orbital, and lattice degrees of freedom [1–5, 22]. The MI transition is accompanied by anomalous changes in the lattice parameters, the average cobalt–oxygen distance *d*(Co–O) in octahedra and pyramids [4, 6,

12, 13], and effective paramagnetic moment μ_{eff} [1, 2], which are determined by changes in the spin states of Co^{3+}. Depending on the relation between the energies of intraatomic exchange and the crystal field, the Co^{3+} ions can be in a low-, intermediate-, or high-spin state. The differences between the spin-state energies in many cobaltites are small and can easily be overcome by temperature changes, which lead to transformation of the spin state of Co and unusual structural and phase transitions (including MI transition) [22].

At present, there is no agreement regarding the spin state of Co^{3+} and the origin of the MI transition in the layered $RBaCo_2O_{5.5}$ cobaltites. The spin state of the Co^{3+} ions in the relatively simple $LaCoO_3$ compound is still unclear and has been the subject of controversy since the 1960s. The situation in the rare-earth layered $RBaCo_2O_{5+\delta}$ cobaltites at $\delta \approx 0.5$ is more complex. First, unlike $LaCoO_3$, the Co^{3+} ions in these compounds can be in two different oxygen environment positions (octahedral, pyramidal). Second, the Co^{3+} ions can also be in the following three different spin states: high-spin (HS, $S = 2$), intermediate-spin (IS, $S = 1$), and low-spin (LS, $S = 0$) states. In addition, the magnetic properties of the $RBaCo_2O_{5+\delta}$ cobaltites depend on a paramagnetic R^{3+} ion [3, 4]. Depending on the type of rare-earth ion, this contribution can be significant, which substantially affects the spin moment of Co^{3+} determined from magnetic measurements.

The authors of the first works [1, 2] assumed that the Co^{3+} ions are in an LS/IS state at low temperatures and evolve to the HS state in both polyhedra at above transition temperature T_{MI} [1, 2]. According to the soft X-ray absorption and the photoelectron spectroscopy of $GdBaCo_2O_{5.5}$, the HS state of the Co^{3+} ions is also retained at $T < T_{MI}$ [23]. The analysis [24] of the X-ray absorption spectra of $TbBaCo_2O_{5.5}$ did not detect a change in the spin state of the Co^{3+} ions at T_{MI}. The Mössbauer spectroscopy of $TbBaCo_2O_{5.5}$ [25] suggests the IS $\rightarrow$ HS transition for the cobalt ions in octahedra and the retained HS state for cobalt in pyramids when temperature increases [25]. Thus, the data obtained are conflicting.

Magnetic methods are most widely used to determine the spin state of Co^{3+} [1, 2]. The complexity of the magnetic methods applied for this purpose is the problem of separating the contribution of the Co^{3+} ions from the PM contribution of rare-earth R^{3+} ions. Moreover, magnetization studies cannot determine the oxygen environment (octahedral or pyramidal) of the Co^{3+} ions. The authors of [4, 7] tried to determine the oxygen environment and the spin state of the Co^{3+} ions using magnetic and structural data. The structural data [4] obtained for $GdBaCo_2O_{5.5}$ revealed elongated octahedra and compressed pyramids in the metallic phase. Since the ionic radius of Co^{3+} increases with the spin state, these results could be interpreted as an increase in the spin state of the Co^{3+} ions in the octahedra and a decrease in the spin state in the pyramids. However, the spin state of the Co^{3+} ions in $GdBaCo_2O_{5.5}$ is LS/IS below T_{MI} and HS/IS above T_{MI} [7], which is in conflict with the structural data [7]. The authors of [4] suppose that the transition into a metallic state is due to a change in the LS state of the Co^{3+} ions to the HS state only in the octahedra without changing the IS state in the pyramids. The same conclusions about the spin state of the Co^{3+} ions in $PrBaCo_2O_{5.5}$ were made without regard for the PM contribution of the Pr^{3+} ions [13]. The authors think that the compression of pyramids can be attributed to either the steric effect or the formation of metallic bonds [4, 13]. This model has received wide acceptance, and many researchers use this model of the MI transition in $RBaCo_2O_{5.5}$.

However, the authors of [26] were doubtful of the reliability of the conclusions [4] regarding the spin state Co^{3+}, since the method of determining the PM contribution of the Gd^{3+} ions that was used in [7] is incorrect (see below). Moreover, the magnetizations of samples [7] were anomalous high as compared to the data in [2, 8]. A method of determining the PM contribution of the Gd^{3+} ions was proposed in [26]. The studies [26] of the magnetization of $GdBaCo_2O_{5.5}$ as a function of temperature and magnetic field showed that the PM contribution of the Gd^{3+} ion almost coincided with the contribution of a free Gd^{3+} ion. As follows from the refined PM contribution of the Gd^{3+} ions, the Co^{3+} ions in $GdBaCo_2O_{5+\delta}$ at $\delta \approx 0.5$ are still in the LS/IS state below T_{MI} and transform into the HS/LS state above T_{MI} [26]. The transition into the metallic state of $GdBaCo_2O_{5.5}$ takes place when the spin state of the Co^{3+} ions increases in the octahedra (LS–HS transition) and decreases in the pyramids (IS–LS transition). These conclusions agree with the structural data obtained by synchrotron X-ray diffraction of $GdBaCo_2O_{5.5}$ [4].

The purpose of this work is to determine the spin state of the Co^{3+} ions in the layered $TbBaCo_2O_{5+\delta}$ cobaltite at $\delta \approx 0.5$. Although the magnetic properties of $TbBaCo_2O_{5.5}$ were extensively studied and the neutron and X-ray diffraction measurements were performed in many works, there are no unambiguous conclusions regarding the spin state of Co^{3+} in this compound in the MI transition range [2, 5, 6, 15, 23–25, 27]. This situation is mainly caused by the fact that the conclusions were drawn using the magnetic data that do not take into account the PM contribution of the Tb^{3+} ions [2, 5]. The spin state of the Co^{3+} ions in $TbBaCo_2O_{5.5}$ in this work is determined with allowance for the PM contribution of the Tb^{3+} ions. As follows from our data, the spin states of the Co^{3+} ions in $TbBaCo_2O_{5.5}$ and $GdBaCo_2O_{5.5}$ near the MI transi-

tion are identical. The Co^{3+} ions are in the LS/IS state below T_{MI} and in the HS/LS state above T_{MI}. The transition to the quasimetallic state occurs when the LS state changes to the HS state in octahedra and IS states to LS states in pyramids in the temperature range $T \approx T_{MI} \pm 50$ K. This assumption explains the increase in the cobalt–oxygen distance d(Co–O) in the octahedra and its decrease in the pyramids in $TbBaCo_2O_{5.5}$ [6] because of the changes in the ionic radii of the Co^{3+} ions induced by changes in their spin state during transition into the metallic phase.

EXPERIMENTAL

Polycrystalline $TbBaCo_2O_{5+\delta}$ samples were synthesized from Tb_4O_7 (99.99% purity), Co_3O_4 (analytical grade), and $BaCO_3$ (special purity grade) powders using solid-phase reactions. The powders taken in the necessary proportion were ground, pressed in pellets, and sintered at 1150°C for 24 h, and the pellets were then cooled to room temperature at a rate of 1 K/min. Oxygen content δ was determined by reducing a sample in a hydrogen atmosphere. The samples were single-phase with $\delta = 0.38$ and had an orthorhombic structure (space group *Pmmm*, no. 47) with unit cell parameters $a = 3.869(5)$ Å, $b = 7.815(4)$ Å, and $c = 7.515(5)$ Å. These results agree with the data in [28]. To change the oxygen content, we annealed the pellets in sealed ampules at a pressure of 5 atm. The Ag_2O compound was as an oxygen source. The linear expansion coefficient was determined using an ULVAC-SINKU RIKO (Japan) quartz dilatometer in the temperature range 77–550 K in the dynamic mode at the rate of change of temperature of 2 K/min. The magnetization was determined on an MPMS-5XL (Quantum Design) device at $T = 10$–400 K and on a 7407 VSM (Lake Shore) vibrating-sample magnetometer at $T = 280$–500 K at the Center for Collective Use of the Institute of Metal Physics.

RESULTS AND DISCUSSION

Figure 1 shows the temperature dependence of the magnetization $M(T)$ of the $TbBaCo_2O_{5.47(2)}$ polycrystal in a magnetic field $H = 1$ kOe. When the temperature decreases below the Curie temperature ($T_C = 279 \pm 2$ K), the magnetization increases sharply, reaches its maximum at $T_{max} \approx 263 \pm 1$ K, and decreases sharply at $T \sim 220$ K. Based on neutron diffraction investigations, the authors of [27] explained this behavior of $M(T)$ in the $TbBaCo_2O_{5.50}$ polycrystal by the formation of a canted FM structure below T_C and its further transition into a noncollinear AFM state. Researchers usually suppose that the transition into the AFM state takes place at $T = T_{max}$, although magnetization is retained within 30–40 K. A gradual transition from a canted FM state into a noncollinear AFM state is likely to occur in the temperature range

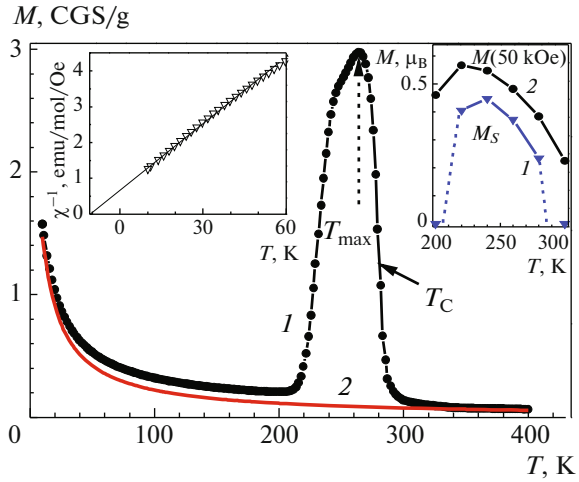

Fig. 1. (Color online) Temperature dependences of the magnetization of $TbBaCo_2O_{5.47}$ (symbols *1*) and the paramagnetic contribution of Tb^{3+} ions (solid line *2*) at $H = 1$ kOe (see text). (left onset) Temperature dependence of the paramagnetic susceptibility at low temperatures. (right inset) temperature dependence of the saturation magnetization M_S and the magnetization of a $TbBaCo_2O_{5.47}$ polycrystal at $H = 50$ kOe.

from $T = T_{max} \sim 260$ K to $T_N \sim 200$ K (Fig. 1). The right inset to Fig. 1 shows the temperature dependences of saturation magnetization M_S, which were obtained extrapolation of $M(H)$ to 50 kOe, and the magnetizations at 50 kOe (PM contribution of the Tb^{3+} ions was subtracted) at $T = 300$–200 K. M_S is seen to decrease below T_{max} and the FM state exists in a narrow temperature range $T \approx 220$–280 K. The increase in the magnetization below $T = 200$ K is explained the PM contribution of the Tb^{3+} ion (Fig. 1, solid line).

At low temperatures in the range $T = 10$–60 K, the paramagnetic susceptibility of the sample (left-side inset to Fig. 1) is described by the Curie–Weiss law with a paramagnetic temperature $\theta_{PM} \approx -11$ K and an effective magnetic moment $\mu_{eff} \approx 8.3\mu_B$, which differs from the moment expected for a free Tb^{3+} ion ($\mu_{eff} = 9.72\mu_B$),

$$\chi \sim \mu_{eff}^2/(T - \theta_{PM}). \quad (1)$$

Rare-earth ion compounds are known to be Van Vleck paramagnets, and their paramagnetic properties are described by the Curie–Weiss law with μ_{eff} of a free ion [29, Chapter 9]. A negative value $\theta_{PM} < 0$ characterizes the presence of AFM interactions and agrees with the AFM ordering of the Tb^{3+} ions in $TbBaCo_2O_{5.5}$ below $\theta_N = 3.44$ K [15].

At present, the influence of the PM contribution of R^{3+} ions on the magnetic properties of $RBaCo_2O_{5+\delta}$ is poorly understood. This contribution was not taken into account in [1, 2, 5, 8, 11, 13, 14, 30], and the

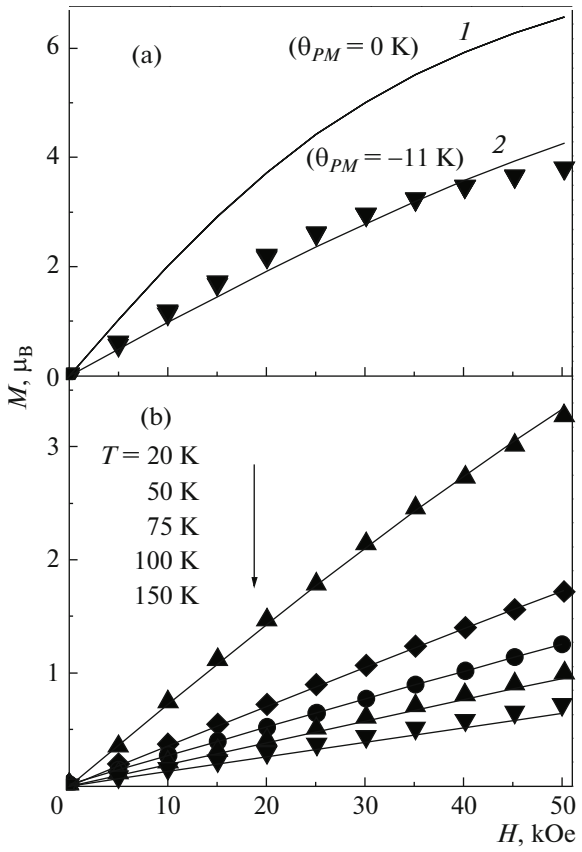

Fig. 2. Field dependences of the magnetization of a $TbBaCo_2O_{5.47}$ polycrystal at T = (a) 10 and (b) 20–150 K. (symbols) Experiment and (solid lines) calculation.

authors of [3, 10, 15, 31] assumed that the contribution of R^{3+} ions coincides with the contribution of a free ion. In [4, 7], the contribution of the Gd^{3+} ion was determined using the results of studying the PM susceptibility of $GdBaCo_2O_{5.5}$ at low temperatures,

$$\chi_{Gd^{3+}}\,[\text{emu/g/Oe}] = 1.92\times10^{-2}/(T+0.4). \qquad (2)$$

This method is inaccurate, since the effective moment depends on the presence of magnetic ions [29]. The value of μ_{eff} in Eq. (2), which differs from the moment of a free Gd^{3+} ion, is caused by the influence of Co ions, as in our experiment for the Tb^{3+} ion (inset to Fig. 1), since the PM susceptibility is determined by the contribution of Co and R^{3+} ions.

To determine the PM contribution of the Gd^{3+} ions, we [26] proposed to use the saturation of magnetization $M(H)$ in a magnetic field at low temperatures. It was preliminarily shown that the contribution of the Co ions to the magnetization of $GdBaCo_2O_{5.5}$ at T = 10 K is low and the field dependence of magnetization at T = 10 K is described by a Brillouin function with the parameters characteristic of the free Gd^{3+} ion at $\theta_{PM} = -1.4$ K,

$$M = N_A g\mu_B J B_S(x), \qquad (3)$$

where $B_S(x)$ is the Brillouin function, N_A is Avogadro's number, $x = g\mu_B JH/k(T-\theta_{PM})$, g is the Landé factor, μ_B is the Bohr magneton, J is the total magnetic moment, H is the magnetic field, and k is the Boltzmann constant.[1] At $x \ll 1$, from Eq. (3) the PM contribution of the Gd^{3+} ions is [26]

$$\chi_{Gd^{3+}}\,[\text{emu/g/Oe}] = 1.57\times10^{-2}/(T+1.4). \qquad (4)$$

Using the method proposed in [26], we determine the PM contribution of the Tb^{3+} ions using the results of studying the magnetization of $TbBaCo_2O_{5.47}$ in the range T = 10–150 K. The symbols in Fig. 2a show the experimental magnetization $M(H)$ of the $TbBaCo_2O_{5.47}$ polycrystal at T = 10 K. Unlike $GdBaCo_2O_{5.52}$ [26], the $M(H)$ dependence of the sample at T = 10 K is not described by Eq. (3) for the parameters of the Tb^{3+} ion at any values of θ_{PM} (Fig. 2a; solid lines *1*, *2*). The $M(H)$ curves at T = 10 K are explained by the fact that $TbBaCo_2O_{5.47}$ at T = 10 K is not a pure paramagnet, since temperature T = 10 K is close to the AFM ordering temperature (θ_N = 3.44 K) of the Tb^{3+} ions [15], in contrast to $GdBaCo_2O_{5.5}$, in which ordering of the Gd^{3+} ions above T = 1.7 K was not detected [3, 4, 10].

The symbols in Fig. 2b show the experimental values of $M(H)$ at T = 20–150 K, which are determined by the total contribution of the Tb^{3+}, Co^{3+}, and 2–3% Co^{2+} ions. The magnetization $M(H)$ determined at T = 10–150 K demonstrates that the PM susceptibility of the Co ions tends to decrease with decreasing temperature (as in $GdBaCo_2O_{5+\delta}$ [26]), which is characteristic of AFM at $T \ll T_{AFM}$ [29]. Our estimates demonstrate that the contribution of the cobalt ions to the magnetization at T = 20 K is at most $0.2\mu_B$. At 20–50 K, the contribution of the Tb^{3+} ion is satisfactorily described by Eq. (3) with Tb^{3+} ion parameters J = 6, g = 1.5, and $\theta_{PM} = -(8 \pm 2)$ K. At T = 75–150 K, the calculated values of $M(H)$ bounded by the contribution of the Co^{3+} ions deviate slightly from the experimental values (Fig. 2b). The contribution of the Tb^{3+} ions to the paramagnetic susceptibility is determined by the following expression derived from Eq. (3) at $x \ll 1$ (T > 300 K and $H \sim$ 10 kOe):

$$\chi\,[\text{emu/mol/Oe}] = C_M/(T-\theta_{PM})[\text{K}], \qquad (5)$$

where $C_M = N_A\mu_B^2\mu_{eff}^2/3k = 11.82$ is the Curie constant for the Tb^{3+} ion [32].

In a wide temperature range of 300–10 K, the PM susceptibility of plain $GdCoO_3$ [33, 34] and $TbCoO_3$ [35] is described by Eq. (5) with the parameters of free

[1] As follows from [13], the field dependence of the magnetization $M(H)$ of the $GdBaCo_2O_{5.5}$ sample studied in [4, 7] is well described by Eq. (3) with the parameters of the free Gd^{3+} ion at $\theta_{PM} = -1$ K.

Gd^{3+} and Tb^{3+} ions, which indirectly supports our conclusions. Line *2* in Fig. 1 shows the PM contribution of the Tb^{3+} ions at $H = 1$ kOe. Our estimates demonstrate that the contribution of the Tb^{3+} ions to the magnetization of $TbBaCo_2O_{5.5}$ above T_{MI} is predominant and the contribution of the Co^{3+} ions accounts for less than 14% of the total magnetization, which is almost half that in $GdBaCo_2O_{5.5}$ [26].

Figure 3 depicts the temperature dependence of the electrical resistivity of $TbBaCo_2O_{5.52}$ at $T = 100$–400 K, which is typical of layered cobaltites [1, 2]. It has a semiconductor character: $\rho(T)$ decreases monotonically with increasing temperature and, in the temperature range 100–250 K, is described by the activation expression

$$\rho(T) \sim \exp(-\Delta E/kT)$$

with an activation energy $\Delta E \approx 40$ meV. An inflection point in the electrical resistivity is observed in the AFM–FM transition range ($T \approx 200$–250 K). This inflection point shifts in a magnetic field toward low temperatures. An unusually high (for cobaltites) magnetoresistance

$$MR_0 = [\rho(H = 15\,\text{kOe}) - \rho(H = 0)]/\rho(H = 0) \approx -12\%$$

is observed in the same temperature range (Fig. 3, bottom insets). Analogous behavior of $\rho(T)$ and MR_0 was detected in $GdBaCo_2O_{5.5}$ [4, 26]. These results are explained by the fact that the carrier mobility in the AFM state is lower than that in the FM state and that a magnetic field widens the temperature range of the FM state toward low temperatures and narrows the range of the AFM state [4]. Below $T \approx T_C \approx 280$ K, the linear dependence $\ln\rho \sim 1/T$ changes and $\rho(T)$ decreases sharply; at $T = 330$–338 K, an electrical resistivity jump takes place, which is thought to be related to a change in the spin state of Co^{3+} (Fig. 3, top inset). Above $T_{MI} \approx 338$ K, the electrical resistivity of the sample weakly depends on temperature, $\rho \sim 2 \times 10^{-3}$ Ω cm (Fig. 3, top inset). The sign of the electrical resistivity derivative $d\rho/dT$ remains negative, which indicates a semiconductor character of $\rho(T)$ in the temperature range up to 400 K.

Figure 4 (left axis) shows the temperature dependence of the experimental PM susceptibility $\chi^{-1}_{exp}(T)$ of the $TbBaCo_2O_{5.52}$ sample measured in a magnetic field $H = 10$ kOe. The $\chi^{-1}_{exp}(T)$ dependence is linear in the range $T = 500$–350 K, a small jump is observed below $T_{MI} \approx 340$ K, and the $\chi^{-1}_{exp}(T)$ is then obviously nonlinear. The value estimated according to the Curie–Weiss law ($\mu_{eff}/Co \approx 7.55\mu_B$) is close to the data in [5] and is too high to be attributed to the spin state of Co^{3+}. To separate the contribution of the Co^{3+} ions from the total magnetization of the sample, we used Eq. (5) to subtract the contribution of the Tb^{3+} ions

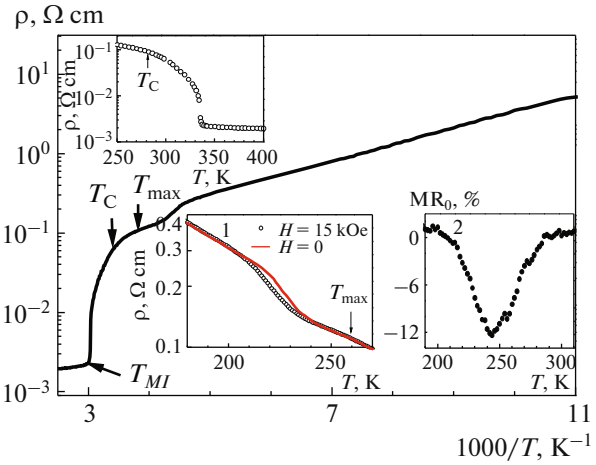

Fig. 3. (Color online) Temperature dependence of the electrical resistivity $\rho(T)$ of a $TbBaCo_2O_{5.52}$ polycrystal. (top inset) $\rho(T)$ near $T_{MI} \sim 338$ K. (bottom insets): (*1*) $\rho(T)$ in the AFM–FM transition range at $H =$ (solid line) 0 and (symbols) 15 kOe and (*2*) temperature dependence of the magnetoresistance at $H = 15$ kOe.

and recalculated $\chi^{-1}(T)$ for the cobalt ions (Fig. 4, right axis). The contribution of the Tb^{3+} ions increases the values of $\chi^{-1}(T)$ in the metallic phase more than sixfold. In the temperature range 500–380 K, inverse susceptibility $\chi^{-1}(T)$ linearly depends on temperature. The nonlinear part of $\chi^{-1}(T)$ is observed below $T \approx 380$ K: $\chi^{-1}(T)$ changes slowly down to $T \approx 350$ K, $\chi^{-1}(T)$ jumps in the range $T_{MI} \approx 345$–335 K, and $\chi^{-1}(T)$ decreases monotonically and nonlinearly when temperature decreases further. A similar change in the slope of $\chi^{-1}(T)$ near T_{MI} was detected in $EuBaCo_2O_{5+\delta}$ crystals (see Fig. 2 in [1]). In the temperature range 500–380 K, the PM susceptibility is described by the Curie–Weiss law with a Néel temperature $\theta_N = -(155 \pm 10$ K) and $\mu_{eff}/Co = 3.28 \pm 0.1\mu_B$; below T_{MI} in the narrow range 325–280 K, $\mu_{eff}/Co = 1.40 \pm 0.05\mu_B$ and $\theta_C = 283 \pm 2$ K are used (Fig. 4b; solid lines μ_{eff} and $\theta_C(\theta_N)$).

No linear segment is detected in the $\chi^{-1}(T)$ dependence in the temperature range 380–280 K, which means that the transition is accompanied by changes in $\mu_{eff}(T)$ with temperature. To test this assumption, we separated linear segments in $\chi^{-1}(T)$ in the temperature range 300–400 K and determined the differential values of μ_{eff} and $\theta_C(\theta_N)$ by the Curie–Weiss law for each segment. The symbols in Fig. 4b show the temperature dependences of the differential values of μ^{diff}_{eff} and $\theta_C(\theta_N)$ thus determined. The MI transition is seen to occur over a wide temperature range (280–380 K): from the maximum ($\mu_{eff}/Co = 3.28 \pm 0.10\mu_B$) at $T =$ 500–380 K to the minimum ($\mu^{diff}_{eff}/Co \approx 0.5\mu_B$) at $T_{MI} \approx 340$ K upon an increase to $\mu^{diff}_{eff}/Co \approx 1.6\mu_B$ at

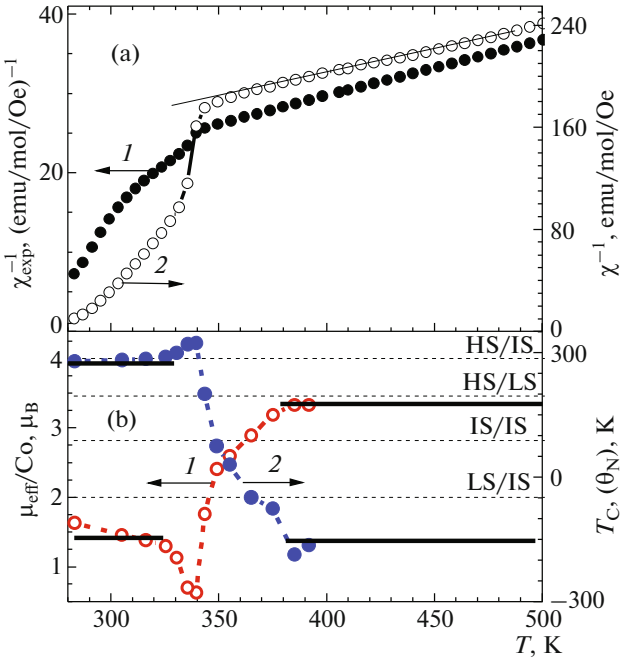

Fig. 4. (Color online) (a): (*1*) Temperature dependence of the paramagnetic susceptibility $\chi_{exp}^{-1}(T)$ of a $TbBaCo_2O_{5.52}$ polycrystal (left axis) and (*2*) $\chi^{-1}(T)$ with subtracted contribution of the Tb^{3+} ion (right axis). (b) Temperature dependences of (solid line *1*) effective moment μ_{eff}/Co and (solid line*2*) temperature $\theta_C(\theta_N)$; (symbols and dashed line) differential values μ_{eff}^{diff}/Co and $\theta_C(\theta_N)$.

$T \sim 280$ K. The behavior of $\theta_C(T)$ is analogous: θ_C increases gradually from $\theta_N \approx -150$ K to $\theta_C \sim +320$ K in the range $T \approx 400-340$ K and then decreases weakly to $\theta_C \approx +280$ K. The values of μ_{eff} and μ_{eff}^{diff} coincide in the range of the linear behavior of $\chi^{-1}(T)$.

In the metallic state ($T = 400-500$ K), the value $\mu_{eff}/Co \approx 3.28 \pm 0.10\mu_B$ corresponds best of all to a mixture of the HS($t_{2g}^4\, e_g^2$, $S = 2$) and LS($t_{2g}^6\, e_g^0$, $S = 0$) states with $\mu_{eff}/Co = 3.43\mu_B$ taken at the proportion 1 : 1 among all possible states of the Co^{3+} ions (Fig. 4b). Below T_{MI} near T_C ($T = 280-325$ K), the value $\mu_{eff}/Co = 1.40 \pm 0.05\mu_B$ means that only up to one-fourth of the Co^{3+} ions are in the IS($t_{2g}^5\, e_g^1$, $S = 1$) state and the remaining ions are in the LS state. The predominance of the fraction of the LS state near T_{MI} in $TbBaCo_2O_{5.5}$ was also detected in [15]. The X-ray and neutron diffraction studies [6, 27] also predicted the existence of an LS/IS state of the Co^{3+} ions below T_{MI}.

Our magnetic data did not allow us to determine the type of oxygen environment of the Co^{3+} ions. The structural investigations [27] of $TbBaCo_2O_{5.5}$ revealed an increase in the oxygen–cobalt bond length d(Co–O) in the octahedra and a decrease in this length in the pyramids in the metallic phase, which can be interpreted as an increase in the ionic radius of Co^{3+} in the octahedra and its decrease in the pyramids. Based on our magnetic data and the structural data in [27], we conclude that the transition into a nonmetallic state is caused by the transition of the HS state into the LS state in the octahedra, as in $GdBaCo_2O_{5.5}$ [26]. In the pyramids, only part (about one-fourth) of the Co^{3+} ions transform from the LS to the IS state, and the remaining ions are still in the LS state (at $T \approx T_C$).

A mixture of Co^{3+} ions with an approximately identical proportion of the IS and LS states is assumed to exist in $GdBaCo_2O_{5.5}$ below T_{MI} [1, 2, 4, 7, 13]. This is partly true: this assumption is likely to be correct for temperatures $T \ll T_{MI}$ [3, 10]. The spontaneous magnetization of $GdBaCo_2O_{5.5}$ without a twinned structure that was determined by extrapolation of the magnetization from high fields increases gradually upon cooling from $M_S \sim 0.3\mu_B$/Co at $T = T_C \approx 280$ K to $M_S \sim 0.6\mu_B$/Co at $T \approx 200$ K (see Figs. 22 and 24 in [3]). At $T = 1.8$ K, it reaches $M_S \sim 1\mu_B$/Co in a magnetic field higher than 300 kOe, which corresponds to the ratio 1 : 1 of the LS/IS states of Co^{3+} at $T \to 0$ [10]. Upon cooling below $T_C \approx 270$ K, the spontaneous magnetization of $GdBaCo_2O_{5.5}$ with a twinned structure increases gradually to $M_S \sim 0.5\mu_B$/Co at $T = 78$ K (see Fig. 3 in [10]). Half of the IS ($S = 1$) spins is parallel to an applied field due to the twinned structure of the crystal and the other half is opposite the field, which leads to the saturation moment $M_S \sim 0.5\mu_B$/Co [3, 10].

As is seen in the inset to Fig. 1, the spontaneous magnetization increases gradually from $M_S \sim 0.11\mu_B$/Co at $T = T_C \approx 280$ K to $M_S \sim 0.23\mu_B$/Co at $T \approx 260$ K. Actually, $M_S \sim 0.11\mu_B$/Co at $T = 280$ K corresponds to the LS/IS state of the Co^{3+} ions at the ratio 0.7 : 0.3 for $T \approx 280$ K, which was obtained above from fitting $\chi^{-1}(T)$ by the Curie–Weiss law. However, the maximum value ($M_S \sim 0.45\mu_B$/Co) is significantly lower than the expected value (about $1\mu_B$/Co) for the LS/IS state at the ratio 1 : 1 because of the twinned and noncollinear FM structure of the $TbBaCo_2O_{5.52}$ crystal.

Therefore, the spin state of Co^{3+} as a function of the type of rare-earth ion R^{3+} is of interest. Using the well-known results on the PM susceptibility of the $RBaCo_2O_{5.5}$ (R = Pr, Nd, Sm, Gd, Tb, Dy, Ho) cobaltites [1, 2, 7, 11–14], we estimated possible spin states of the Co^{3+} ions near the MI transition with allowance for the PM contribution of the R^{3+} ions. For simplicity, the PM contribution was assumed to coincide with the contribution of a free R^{3+} ion [3]. Using these estimates, we can assume that the Co^{3+} ions in all these cobaltites below T_{MI} are in an IS/LS state.

The Co^{3+} ions in the metallic phase in all cobaltites except for those with R = Ho and Pr are in an HS/LS state.[2]

Anomalous lattice expansion is detected along with the spin transition (Fig. 5). The thermal expansion was measured on a $TbBaCo_{1.96}O_{5+\delta}$ single crystal along three directions in a 3 × 3 × 2.5 mm^3 parallelepiped. One parallelepiped axis is perpendicular to axis *c* and coincides with the [120] growth direction, and two other axes are directed along axis *c*.

The symbols in Fig. 5 show the temperature dependence of the volumetric expansion $\Delta V/V$ near $T \approx T_{MI} \pm 100$ K. The volumetric expansion coefficient $\alpha_V(T) = 1/V \cdot dV/dT$ in the metallic phase (400–500 K) is higher than that in the dielectric phase ($T < T_C$), 3.9×10^{-5} and 3.2×10^{-5} K^{-1}, respectively. The deviations of $\Delta V/V(T)$ from the linear dependence of the lattice (solid lines) take place at $T \approx T_{MI} \pm 40$ K and are indicated by arrows. The nonmonotonic (S-like) change in the lattice volume $\Delta V/V(T)$ at the transition range is noteworthy: the lattice volume decreases upon heating above $T \approx 300$ K, increases sharply at $T \approx T_{MI} \pm 10$ K, and then again decreases. The linear expansion $\Delta L/L(T)$ near T_{MI} also exhibits nonmonotonic (S-like) behavior (Fig. 5, top inset). An analogy between $\Delta V/V(T)$ and $\mu_{eff}^{diff}(T)$ in Fig. 4b is visible. The results of thermal expansion are likely to reflect the fact of different temperature changes in the spin states of the Co^{3+} ions in different polyhedra near the MI transition. The linear expansion $\Delta L/L(T)$ has an anisotropic character (Fig. 5, left inset). During the transition into the metallic state, the lattice expands along axis *c* and is compressed along [120] normal to axis *c*. The lattice expansion $\Delta L/L(T)$ along axis *c*, the lattice compression normal to axis *c*, and the increase in the volume $\Delta V/V$ during the transition into the metallic phase agree qualitatively with the neutron diffraction data in [5, 6]. The linear and volumetric expansion curves plotted upon heating and cooling exhibit hysteretic behavior, supporting the fact that the MI transformation is a first-order phase transition.

The temperature dependence of the linear thermal expansion coefficient $\alpha(T) = 1/L \cdot dL/dT$ of $TbBaCo_{1.96}O_{5+\delta}$ has a well-pronounced peak at $T = T_{MI} \approx$ 338–340 K and a weak anomaly at $T_N \approx 190$ K (Fig. 5, bottom inset). A good correlation between the linear thermal expansion coefficient $\alpha(T)$ and the effective magnetic moment $\mu_{eff}(T)$ is clearly visible (Fig. 4b). Coefficient $\alpha(T)$ deviates from the linear temperature dependence (solid lines) induced by thermal lattice expansion in the range $T \approx 380$–290 K, i.e., the temperature range of changing the spin state of Co^{3+}.

[2] As follows from [13], the Co^{3+} ions in the metallic phase of $PrBaCo_2O_{5.50}$ are in an HS/IS state at the ratio 1 : 1 if the PM contribution is taken into account.

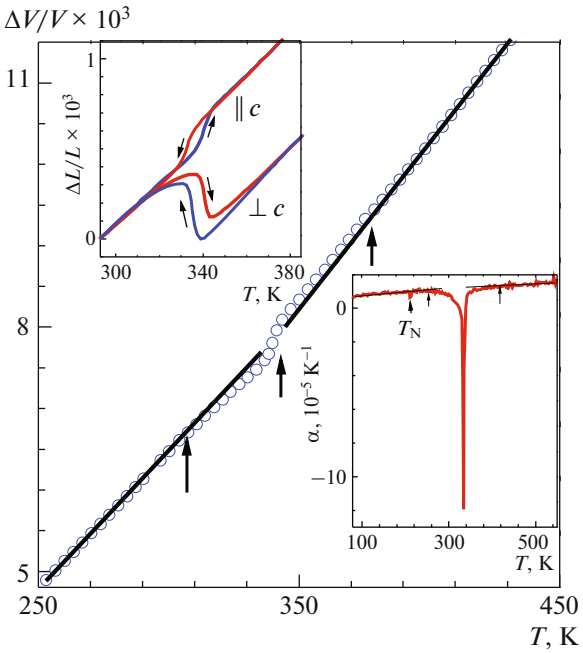

Fig. 5. (Color online) Temperature dependence of the volumetric expansion $\Delta V/V$ of a $TbBaCo_2O_{5+\delta}$ single crystal. (insets) Temperature dependences of the linear expansion $\Delta L/L$ (along and across axis *c*, upon heating and cooling) at T_{MI} and linear thermal expansion coefficient $\alpha(T)$ along the [120] direction.

The $\alpha(T)$ anomaly at $T_N \approx 190$ K is smaller than $\alpha(T)$ at T_{MI} by almost two orders of magnitude, which excludes the possibility of its explanation by changing the spin state of the Co^{3+} ions near this temperature. Allowing for the magnetic data (Fig. 1), we assume that this anomaly can be caused by magnetostriction phenomena during the transition from a canted FM state to a noncollinear AFM state. The thermal expansion of $TbBaCo_{1.96}O_{5+\delta}$ confirms the retention of the LS/IS state of the Co^{3+} ions at low temperatures down to at least $T = 80$ K.

Extrapolating the thermal expansion of nickel below and above the transition temperature, we estimated the increase in the unit cell volume during the MI transition at $\Delta V/V \approx 2 \times 10^{-4}$ at T_{MI}. Approximately the same value of $\Delta V/V$ was obtained for a $GdBaCo_2O_{5.5}$ polycrystal [36]. Volume increment $\Delta V/V$ near T_{MI} demonstrates that the transition into a metallic state is accompanied by an increase in the spin state of the Co^{3+} ions. The results of studying the thermal expansion of a $TbBaCo_{1.96}O_{5+\delta}$ single crystal support the fact that the spin state of Co^{3+} changes over a wide temperature range $T \approx T_{MI} \pm$ (40–50) K. The physical properties, such as $\rho(T)$ (Fig. 3), $\chi^{-1}(T)$ (Fig. 4), $\alpha(T)$, $\Delta L/L$, and $\Delta V/V$ (Fig. 5), change

sharply only in a narrow temperature range $T = T_{MI} \pm 10$ K, where $\chi^{-1}(T)$ and μ_{eff} change jumpwise.

CONCLUSIONS

Magnetic and structural investigations are the main methods for determining the spin state of the Co^{3+} ions in the layered $RBaCo_2O_{5.5}$ cobaltites near the MI transition. However, unambiguous conclusions regarding the spin state of the Co^{3+} ions cannot always be drawn using the results of these investigations, which is mainly caused by the fact that conclusions were usually based on the magnetic data that incorrectly took into account the PM contribution of the R^{3+} ions. In this work, we studied the magnetization of $TbBaCo_2O_{5.5}$ over a wide temperature range and found that the PM contribution of the Tb^{3+} ions was determined by the Curie–Weiss law with the parameters of a free Tb^{3+} ion at $\theta_{PM} = -8 \pm 2$ K. The spin states of the Co^{3+} ions in $TbBaCo_2O_{5.5}$ and $GdBaCo_2O_{5.5}$ were found to be identical with allowance for the PM contribution of the Tb^{3+} ions. The Co^{3+} ions are in an HS/LS state above T_{MI} and in an LS/IS state below T_{MI}. The transition into a metallic state takes place when the Co^{3+} ions in the octahedra transform from the LS to the HS state and the Co^{3+} ions in the pyramids transform from the IS to the LS state, according to the structural data indicating expansion of the octahedra and compression of the pyramids. As follows form the data obtained for volumetric and linear expansion, the MI transition occurs over a wide temperature range $T \approx T_{MI} \pm (40–50)$ K when the spins state of the Co^{3+} changes. The hysteretic behavior of the volumetric and linear expansion demonstrates that the MI transition in the compound under study is a first-order phase transition. Thermal expansion data indicate that the LS/IS state of the Co^{3+} ions is retained down to $T = 80$ K.

NOTE ADDED IN PROOF (FEBRUARY 13, 2020)

In conclusion, we note that the authors of [5, 12, 37, 38] considered the role of orbital ordering in the metal–insulator transition in layered cobaltites. Neutron diffraction of $TbBaCo_2O_{5+\delta}$ at $\delta = 0.5$ [37] and X-ray diffraction of $GdBaCo_2O_{5.5}$ [38] demonstrate that the spin states of the Co^{3+} ions differ in the low-temperature phase and they are located in two different octahedra and two different pyramids because of orbital ordering. It is assumed that, in the low-temperature $TbBaCo_2O_{5+\delta}$ at $\delta = 0.5$ and $T = 260$ K, the Co^{3+} ions in octahedra are in the LS state and half the ions in pyramids is in the HS state and the other half is in the LS state [37].

The increase in μ_{eff}/Co approximately from $0.5\mu_B$ to $1.5\mu_B$ when temperature decreases from T_{MI} to T_C in both $TbBaCo_2O_{5+\delta}$ at $\delta \approx 0.5$ (see Fig. 4) and $GdBaCo_2O_{5+\delta}$ at $\delta \approx 0.5$ (see Fig. 5 in [26]) is thought to be caused by an increase in the fraction of the IS state from a few percent to 20–25% in the IS/LS state of the pyramids. The same $\mu_{eff}/Co(T)$ results could also be interpreted as an increase in the fraction of HS in the HS/LS state of the pyramids; the only difference is that the fraction of HS states would be approximately half as much. In the orbital ordering model approximation, the transition into the low-temperature insulator state occurs from the HS into the LS state of the Co^{3+} ions in octahedra. In pyramids, half the Co^{3+} ions is retained in the LS state and the other half should transform into the HS state. This model is in conflict with our data and the well-known data [15] on measuring the paramagnetic susceptibility, since the effective moment in the low-temperature phase should be twice as large, about $\mu_{eff}/Co \approx 2.5\mu_B$. On the other hand, the authors of [15] state that the magnetic moment per Co^{3+} ion increases from $1.22\mu_B$ to $2.8\mu_B$ when the magnetic field increases from 1 to 50 kOe. The substantiation of the proposed model and, in particular, the presence of the HS state in the low-temperature phase need additional investigations.

ACKNOWLEDGMENTS

We thank A.V. Korolev and D.A. Shishkin for the magnetic measurements, as well as A.V. Telegin for fruitful discussion.

FUNDING

This work was performed in terms of a state assignment of the Federal Agency of Scientific Organizations, project Spin no. AAAA-A18-118020290104-2. This work was supported in part by the Russian Foundation for Basic Research (project 20-02-00461).

REFERENCES

1. C. Martin, A. Maignan, D. Pelloquin, et al., Appl. Phys. Lett. **71**, 1421 (1997).
2. A. Maignan, C. Martin, D. Pelloquin, et al., J. Solid State Chem. **142**, 247 (1999).
3. A. A. Taskin, A. N. Lavrov, and Yoichi Ando, Phys. Rev. B **71**, 134414 (2005).
4. C. Frontera, J. L. García-Muñoz, A. Llobet, et al., Phys. Rev. B 65, 180405(R) (2002).
5. Y. Moritomo, T. Akimoto, M. Takeo, et al., Phys. Rev. B 61, 13325(R) (2000).
6. H. Kusuya, A. Machida, Y. Moritomo, et al., J. Phys. Soc. Jpn. **70**, 3577 (2001).
7. M. Respaud, C. Frontera, J. L. García-Muñoz, M. A. Aranda, B. Raquet, J. M. Broto, H. Rakoto, M. Goiran, A. Llobet, and J. Rodriguez-Carvajal, Phys. Rev. B **64**, 214401 (2001).
8. S. Roy, M. Khan, Y. Q. Guo, et al., Phys. Rev. B **65**, 064437 (2002).

9. F. Fauth, E. Suard, V. Caignaert, et al., Phys. Rev. B **66**, 184421 (2002).
10. Z. X. Zhou, S. McCal., C. S. Alexander, et al., Phys. Rev. B **70**, 024425 (2004).
11. H. D. Zhou and J. B. Goodenough, J. Solid State Chem. **177**, 3339 (2004).
12. E. Pomjakushina, K. Conder, and V. Pomjakushin, Phys. Rev. B **73**, 113105 (2006).
13. C. Frontera, J. L. García-Muñoz, A. E. Carillo, et al., Phys. Rev. B **74**, 054406 (2006).
14. Y. Diaz-Fernandez, L. Malavasi, and M. C. Mozzati, Phys. Rev. B **78**, 144405 (2008).
15. M. Baran, V. I. Gatalskaya, R. Szymczak, et al., J. Phys.: Condens. Matter **15**, 8853 (2003).
16. E. L. Nagaev, Phys. Usp. **39**, 781 (1996).
17. E. Dagotto, New J. Phys. **7**, 67 (2005).
18. N. I. Solin, J. Magn. Magn. Mater. **401**, 677 (2016).
19. V. A. Ryzhov, A. V. Lazuta, V. P. Khavronin, P. L. Molkanov, Ya. M. Mukovskii, and A. E. Pestun, Phys. Solid State **56**, 68 (2014).
20. N. I. Solin, S. V. Naumov, S. V. Telegin, et al., JETP Lett. **104**, 49 (2016).
21. N. I. Solin, S. V. Naumov, and S. V. Telegin, J. Exp. Theor. Phys. **128**, 281 (2019).
22. N. B. Ivanova, S. G. Ovchinnikov, M. M. Korshunov, I. M. Eremin, and N. V. Kazak, Phys. Usp. **52**, 789 (2009).
23. Z. Hu, Hua Wu, T. C. Koethe, et al., New J. Phys. **14**, 123025 (2012).
24. M. Hidaka, M. Soejima, R. P. Wijesundera, et al., Phys. Status Solidi B **243**, 1813 (2006).
25. M. Kopcewicz, D. D. Khalyavin, I. O. Troyanchuk etal., J. Phys.: Condens. Matter **14**, 9007 (2002).
26. N. I. Solin, S. V. Naumov, and S. V. Telegin, JETP Lett. **107**, 203 (2018).
27. M. Soda, Y. Yasui, T. Fujita, et al., J. Phys. Soc. Jpn. **72**, 1729 (2003).
28. E. Rautama and M. Karppinen, J. Solid State Chem. **83**, 1102 (2010).
29. S. V. Vonsovskii, *Magnetism* (Wiley, New York, 1971).
30. T. I. Arbuzova, S. V. Telegin, S. V. Naumov, et al., Solid State Phenom. **215**, 83 (2014).
31. S. Kolesnik, B. Dabrowski, O. Chmaissem, et al., Phys. Rev. B **86**, 1064434 (2012).
32. J. S. Smart, *Effective Field Theories of Magnetism* (Saunders, London, 1966).
33. V. A. Dudnikov, D. A. Velikanov, N. V. Kazak, C. R. Michel, J. Bartolome, A. Arauzo, S. G. Ovchinnikov, and G. S. Patrin, Phys. Solid State **54**, 79 (2012).
34. N. B. Ivanova, N. V. Kazak, C. R. Michel, A. D. Balaev, and S. G. Ovchinnikov, Phys. Solid State **49**, 2126 (2007).
35. A. Muñoz, M. Martínez-Lope, J. A. Alonso, et al., Eur. J. Inorg. Chem. **2012**, 5825 (2012).
36. K. R. Zhdanov, M. Yu. Kameneva, L. P. Kozeeva, and A. N. Lavrov, Phys. Solid State **52**, 1688 (2010).
37. V. P. Plakhty, Y. P. Chernenkov, S. N. Barilo, et al., Phys. Rev. B **71**, 214407 (2005).
38. M. García-Fernandes, V. Scarnoli, U. Staub, et al., Phys. Rev. B **78**, 054424 (2008).

Translated by K. Shakhlevich